2018 Annual American Control Conference (ACC)
June 27–29, 2018. Wisconsin Center, Milwaukee, USA

Synchronizing and Desynchronizing Neural Populations through Phase Distribution Control

Bharat Monga[1] and Gary Froyland[2] and Jeff Moehlis[3]

Abstract— **In this article, we devise two related control algorithms to change the degree of synchrony of a population of noise-free, identical, uncoupled neural oscillators using a single control input. The algorithms are based on phase reduction, and use a population-level partial differential equation formulation to change the phase distribution of the neurons as desired. Motivated by the pathological neural synchronization hypothesized to be present in patients suffering from essential and parkinsonian tremor, we take our control objective to be the desynchronization of an initially synchronized neural population. Through numerical simulations, we are able to show that our algorithms work for both Type I and Type II neural populations. To demonstrate the versatility of our control algorithms, we also show that they can be applied to synchronize an initially desynchronized neural population as well. For the systems considered in this paper, the control algorithms can be applied to achieve any desired traveling-wave neural phase distribution, as long as the combination of initial and desired phase distributions is non-degenerate.**

I. INTRODUCTION

Synchronization of neural activity holds significant biological relevance. It is crucial for visual and odor processing [1], [2], and also in learning and memory recall [3], [4]. However, synchronization can be detrimental as well. For example, pathological neural synchronization in the thalamus and the STN brain region is hypothesized to be one of the causes of motor symptoms for essential and parkinsonian tremor, respectively [5], [6]. Therefore, a number of researchers have proposed control techniques to either synchronize or desynchronize neural activity; see, e.g., [7], [8], [9], [10], [11].

Phase reduction, a classical reduction technique based on isochrons [12], has been instrumental in the development of many of these control algorithms. Phase reduction reduces the dimensionality of a dynamical system with a periodic orbit to a single phase variable, and captures the oscillator's phase change due to an external perturbation through the phase response curve (PRC). This can make the analysis of high dimensional systems more tractable, and their control [13], [11], [14], [15], [16], [17] experimentally implementable; see e.g., [18], [19], [20], [14].

[1]Bharat Monga is a Doctoral candidate in the Department of Mechanical Engineering, University of California Santa Barbara, Santa Barbara CA 93106, USA monga@ucsb.edu

[2]Gary Froyland is a faculty in the School of Mathematics and Statistics, University of New South Wales, Sydney NSW 2052, Australia g.froyland@unsw.edu.au

[3]Jeff Moehlis is a faculty in the Department of Mechanical Engineering, University of California Santa Barbara, Santa Barbara CA 93106, USA moehlis@engineering.ucsb.edu

Motivated by the pathological synchronization present in patients suffering from parkinsonian and essential tremor, in this article we devise and compare two closely related control algorithms to desynchronize a neural population. We note that previously proposed algorithms based on individual neuron models [13], [21], [22], [11] can face implementation challenges if they require observability of phases of all neurons at all times [22], or demand initial phases to be sufficiently close [11], [15]. There are also population-level algorithms for desynchronization in the literature which use multiple inputs [23], [9], [15], making experimental implementation difficult because they require multiple electrodes to be implanted in a small region of brain tissue.

Our algorithms overcome these difficulties, as they are based on a population-level model, and require a single control input. They use a partial differential equation (PDE) formulation to change an initial probability distribution of phases of a neural population as desired. Thus, to desynchronize an initially synchronized neural population, we start with a single-hump probability distribution, and set the final distribution to be a uniform probability distribution. We demonstrate this for both Type I and Type II neural populations. Note that our algorithms are very versatile, and are not dependent on the choice of an initial distribution: they can be applied to obtain any desired traveling-wave neural phase probability distribution, as long as the combination of the initial and the desired phase distributions is not degenerate. Therefore, our algorithms can work in the other direction, i.e., they can be used to synchronize an initially desynchronized neural population as well.

This article in organized as follows. In Section II, we give background on phase reduction and the partial differential equation for the phase probability distribution. In Section III, we devise the control algorithms to achieve the desired neural population distribution. In Section IV we compare the simulation results of our control algorithms. Section V concludes the article by highlighting the implications of the results.

II. BACKGROUND

In this section, we give background on the key concepts of phase reduction, phase response curves, and the partial differential equation for the evolution of the phase density. These will be crucial for the formulation of our control algorithms in Section III.

978-1-5386-5427-9/$31.00 ©2018 AACC

A. Phase Reduction

Phase reduction is a classical technique to describe the dynamics near a periodic orbit. It works by reducing the dimensionality of a dynamical system to a single phase variable θ [24], [25]. Consider a general n-dimensional dynamical system given by

$$\frac{d\mathbf{x}}{dt} = F(\mathbf{x}), \qquad \mathbf{x} \in \mathbb{R}^n, \qquad (n \geq 2). \tag{1}$$

Suppose this system has a stable periodic orbit $\gamma(t)$ with period T. For each point $\mathbf{x}^*$ in the basin of attraction of the periodic orbit, there exists a corresponding phase $\theta(\mathbf{x}^*)$ such that

$$\lim_{t\to\infty} \left| \mathbf{x}(t) - \gamma\left(t + \frac{T}{2\pi}\,\theta(\mathbf{x}^*)\right)\right| = 0, \tag{2}$$

where $\mathbf{x}(t)$ is the flow of the initial point $\mathbf{x}^*$ under the given vector field. The function $\theta(\mathbf{x})$ is called the *asymptotic phase* of $\mathbf{x}$, and takes values in $[0, 2\pi)$. For neuroscience applications, we typically take $\theta = 0$ to correspond to the neuron firing an action potential. *Isochrons* are level sets of this phase function, and it is typical to define isochrons so that the phase of a trajectory advances linearly in time both on and off the periodic orbit, which implies that

$$\frac{d\theta}{dt} = \frac{2\pi}{T} \equiv \omega \tag{3}$$

in the entire basin of attraction of the periodic orbit. Now consider the system

$$\frac{d\mathbf{x}}{dt} = F(\mathbf{x}) + U(t), \qquad \mathbf{x} \in \mathbb{R}^n, \tag{4}$$

where $U(t) \in \mathbb{R}^n$ is an infinitesimal control input. Phase reduction can be used to reduce this system to a one dimensional system given by [26]:

$$\dot{\theta} = \omega + U(t)^T \mathcal{Z}(\theta). \tag{5}$$

Here $\mathcal{Z}(\theta) \equiv \nabla_{\gamma(t)}\theta \in \mathbb{R}^n$ is the gradient of phase variable θ evaluated on the periodic orbit and is referred to as the *(infinitesimal) phase response curve (PRC)*. It quantifies the effect of an infinitesimal control input on the phase of a periodic orbit.

B. Phase density equation

Given a population of noise-free, identical, uncoupled oscillators all receiving the same control input, it is convenient to represent the population dynamics in terms of its probability distribution $\rho(\theta, t)$, with the interpretation that $\rho(\theta, t)d\theta$ is the probability that a neuron's phase lies in the interval $[\theta, \theta + d\theta)$ at time t. This evolves according to the advection equation [26], [15]

$$\frac{\partial \rho(\theta,t)}{\partial t} = -\frac{\partial}{\partial \theta}\left[\left(\omega + U(t)^T \mathcal{Z}(\theta)\right)\rho(\theta,t)\right]. \tag{6}$$

The desired final probability distribution $\rho_f(\theta, t)$ will be taken to be a traveling wave which evolves according to

$$\frac{\partial \rho_f(\theta,t)}{\partial t} = -\omega \frac{\partial \rho_f(\theta,t)}{\partial \theta}. \tag{7}$$

Note that (7) is of the same form as (6) with $U = 0$.

In the next section, we will show how these two equations can be used to devise our control algorithms.

III. Control Algorithm

In this section, we devise two related control algorithms to change synchrony of a neural population. We do this by directly working with the partial differential equation (6) which governs the evolution of the phase distribution of the population. Although we focus on desynchronization in this article, the algorithms are not restricted to achieving this particular control objective. The algorithms can be applied to a network of noise-free, identical, uncoupled oscillators to achieve any desired traveling-wave probability distribution.

Our approach is to select the control $U(t)$ at each time instant so that the L^2 difference between the current density $\rho(\theta, t)$ and the final target density $\rho_f(\theta, t)$ is instantaneously decreased as much as possible subject to the control limits. This method is similar in spirit to approaches used in optimal mixing of fluids. For example, [27] considers the problem of selecting a velocity field that will instantaneously mix a given tracer density as rapidly as possible toward a uniform tracer density. They do this by computing the time derivative of the square of L^2 norm of the spatial derivative of the concentration field, and minimizing this quantity. In discrete time, [28] considers fixed aperiodic advective dynamics and asks how to push a given tracer density as close as possible toward a target density by optimally selecting local stochastic perturbations at each time step. This problem is posed as a convex quadratic optimization problem, minimizing the square of the L^2 distance between the target density and the tracer density one time unit in the future.

To devise our control laws, we define the L^2 norm of the probability distribution difference as

$$V(t) = \int_0^{2\pi} \left(\rho(\theta,t) - \rho_f(\theta,t)\right)^2 d\theta. \tag{8}$$

The L^2 norm is positive over the range of all probability distributions, except being zero when $\rho(\theta, t) = \rho_f(\theta, t)$. Its time derivative is given as

$$\begin{aligned}
\dot{V}(t) &= \int_0^{2\pi} \frac{\partial}{\partial t}\left(\rho(\theta,t) - \rho_f(\theta,t)\right)^2 d\theta \\
&= \int_0^{2\pi} 2\left(\rho(\theta,t) - \rho_f(\theta,t)\right)\left(\frac{\partial \rho}{\partial t} - \frac{\partial \rho_f}{\partial t}\right) d\theta \qquad (9) \\
&= -2\int_0^{2\pi} \left(\rho(\theta,t) - \rho_f(\theta,t)\right) \\
&\qquad \times \frac{\partial}{\partial \theta}\left[\left(\omega + U(t)^T\mathcal{Z}(\theta)\right)\rho(\theta,t) - \omega\rho_f(\theta,t)\right] d\theta \\
&= -2\omega\int_0^{2\pi} \left(\rho(\theta,t) - \rho_f(\theta,t)\right)\frac{\partial}{\partial\theta}\left(\rho(\theta,t) - \rho_f(\theta,t)\right) d\theta \\
&\quad - 2\int_0^{2\pi} \left(\rho(\theta,t) - \rho_f(\theta,t)\right) U^T(t)\frac{\partial}{\partial\theta}\left(\mathcal{Z}(\theta)\rho(\theta,t)\right) d\theta \\
&= 2\int_0^{2\pi} \left(\frac{\partial \rho}{\partial\theta} - \frac{\partial\rho_f}{\partial\theta}\right) U(t)^T\mathcal{Z}(\theta)\rho(\theta,t) d\theta. \qquad (10)
\end{aligned}$$

Here, the first equality follows from the Leibniz rule from elementary calculus, and the last equality follows from the previous line by applying integration by parts and imposing periodic boundary conditions. Therefore,

$$\dot{V}(t) = U^T(t) I(t), \tag{11}$$

where $I(t) \in \mathbb{R}^n$ is given by the integral

$$I(t) = 2 \int_0^{2\pi} \left(\frac{\partial \rho(\theta,t)}{\partial \theta} - \frac{\partial \rho_f(\theta,t)}{\partial \theta} \right) \mathcal{Z}(\theta) \rho(\theta,t) d\theta. \tag{12}$$

Then by taking control input $U(t) = -KI(t)$, where $K \in \mathbb{R}^n \times \mathbb{R}^n$ is a symmetric positive definite matrix, we get the time derivative of the L^2 norm, $\dot{V}(\rho, \rho_f, t) = -I(t)^T K I(t)$ as negative definite. Thus, the control law $U(t) = -KI(t)$ will decrease the L^2 norm until the current probability distribution becomes equal to the desired distribution. Note that we have assumed $I(t) \neq 0$, unless $\rho(\theta,t) = \rho_f(\theta,t)$. We do not consider degenerate cases where $I(t) = 0$ for $\rho(\theta,t) \neq \rho_f(\theta,t)$ in this paper. Such degeneracy can be avoided by modifying the initial or the desired distribution slightly, without compromising the control objective.

For both experimental and numerical reasons, it is more practical to have a bounded control input, so we take a "clipped" proportional control law

$$U_p(t) = \max\left(\min\left(U_{max}, -KI(t)\right), U_{min}\right). \tag{13}$$

Here U_{max} and U_{min} are column vectors whose elements are the upper and lower bounds of the control input vector, respectively. The max, and min operators find the maximum and minimum of 2 vectors element-wise, respectively.

We can also define a bang-bang control law

$$U_{b,i}(t) = \begin{cases} U_{min,i}, & I_i(t) > 0 \\ U_{max,i}, & I_i(t) < 0 \end{cases}, \; i = 1, 2, \ldots, n. \tag{14}$$

Here $U_{b,i}$, $U_{min,i}$, $U_{max,i}$, and $I_i(t)$ represent the ith elements of the corresponding vectors. Thus for a bang-bang control law, the control input is always at its maximum or minimum allowable limit.

Note that for both of these control laws (equations (13) and (14)), the time derivative of the L^2 norm is still negative definite. But with the bang-bang control, the decay rate of the L^2 norm is more negative than that in proportional control. So in theory, one expects the L^2 norm to converge to 0 faster with the bang-bang control. However, as we will see in Section IV, this is not the case, as bang-bang control can lead to a rapidly changing control input when the problem is discretized for numerical simulations.

IV. Simulation Results

In this section, we apply the control laws devised in the previous section to desynchronize an initially synchronized neural population. To demonstrate the versatility of our algorithms, we will also show that our control algorithms work in the other direction as well, i.e., in synchronizing an initially desynchronized neural population.

Here we consider underactuated dynamical systems with only one degree of actuation: the control input vector is $U(t) = [u(t),\ 0, \ldots, 0]^T$. We make this assumption because in most conductance-based models of neurons, we can only give a single control input in the form of a current to one of the elements of the state vector, which corresponds to the voltage across the cell membrane. This assumption reduces the control vectors ($KI(t)$, $U_p(t)$, $U_b(t)$, U_{max}, U_{min}) from Section III into the corresponding scalars ($kI(t)$, $u_p(t)$, $u_b(t)$, u_{max}, u_{min}), respectively. Note that, only the first component of PRC $\mathcal{Z}_1(\theta)$ comes into picture in the control input. From here onward, whenever we refer to the PRC, we mean only the first component of the n-dimensional PRC.

The initial probability distribution is taken to have a single hump, corresponding to (partial) synchronization; since this needs to be periodic in θ, we take it to be a von Mises distribution

$$\rho(\theta, 0) = \frac{e^{b\cos(\theta - \mu)}}{2\pi \mathcal{I}_0(b)}, \tag{15}$$

with $\mathcal{I}_0(b)$ the modified Bessel function of first kind of order 0. We take $b = 26$, and the mean $\mu = \pi$ in our simulations. The desired final distribution is taken as $\rho_f(\theta,t) = 1/(2\pi)$, i.e., a uniform distribution, corresponding to complete desynchronization.

To numerically compute the solution of the PDEs (6) and (7), the former with control inputs given by (13) and (14), we use a method of lines type approach, where the spatial derivative (right hand side of equation (6) and (7)) is discretized by a backward difference scheme, and the resulting ODEs are solved by a 3rd order total variation diminishing Runge-Kutta method [29], [30]. We use periodic boundary conditions at the boundaries of the spatial domain. For the proportional control, we choose an optimum value of k, giving best numerical results.

Note that the proportional control input is large initially, when the desired and current phase distributions are quite different. With time, control input becomes small, as the two distributions become more similar. So if we choose a small k value, the proportional control would be effective in decreasing the L^2 norm only initially. If we choose a large k value, the proportional control would behave more like the bang-bang control initially due to clipping of the large control input, which makes the control less effective (we will see later on that bang-bang control is less effective than the proportional control). So we settle for an "in between" k value, which overall does a good job of reducing the L^2 norm.

If the PRC is positive for all values of θ, i.e., a positive perturbation always advances the phase of the oscillator, the PRC is labeled as being Type I [31]. On the other hand, if a positive perturbation can both delay and advance the phase, i.e., the PRC has both negative and positive regimes, the PRC is classified as Type II. Type I and Type II PRCs are associated with Type I and Type II neuron models respectively, which are known to have distinctive dynamics [26]. With this in mind, we will test our algorithm for both Type I and Type II neural populations.

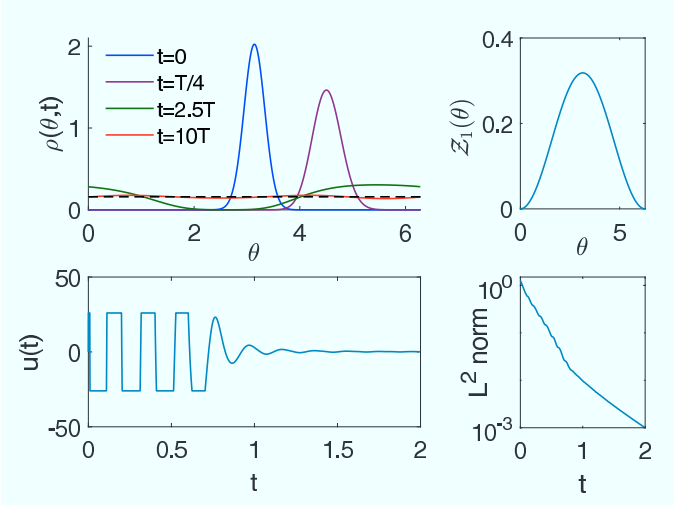

Fig. 1. Proportional control for a Type I neural population going from a synchronized to a desynchronized state; here $k = 10000$. In the top left panel, the colored (resp., black dashed) lines shows the probability distribution $\rho(\theta, t)$ (resp., $\rho_f(\theta, t)$) at various times. The top right panel shows the PRC, while the bottom panels show the control input and the L^2 norm (8) for the difference between the actual and desired distributions on a logarithm scale. The period $T = 0.2$ s.

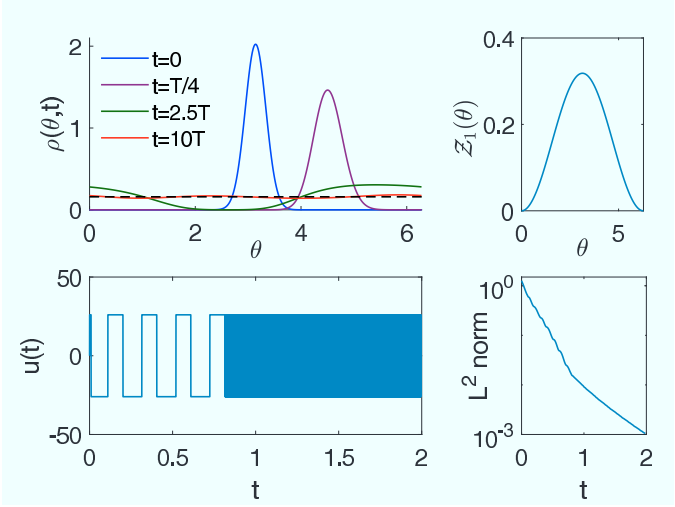

Fig. 2. Bang-bang control for a Type I neural population going from a synchronized to desynchronized state. In the top left panel, the colored (resp., black dashed) lines shows the probability distribution $\rho(\theta, t)$ (resp., $\rho_f(\theta, t)$) at various times. The top right panel shows the PRC, while the bottom panels show the control input and the L^2 norm (8) on a logarithm scale. The period $T = 0.2$ s.

A. Type I neural population

Type I neuron models typically bifurcate to an oscillatory regime through a Saddle Node on an Invariant Circle (SNIC) bifurcation [31]. As the PRC is known to be proportional to $1 - \cos(\theta)$ for a SNIC bifurcation [31], we take the PRC to be $(1 - \cos(\theta))/(2\pi)$ as an example. Note that the PRC is always positive. We take the time period of the oscillator as $T = 0.2$ s, spatial grid size $d\theta = \pi/200$ rad, and time grid size $dt = 0.0005$. We simulate equations (6) and (7) with both proportional control (13) and bang-bang control (14), with $k = 10000$, $u_{max} = -u_{min} = 26$. Results for proportional and bang-bang control are shown in Figures 1 and 2, respectively.

We see that the both proportional and bang-bang control are able to transform the probability distribution into a uniform distribution over 10 time periods of the oscillator. To reach an L^2 norm of 0.001 for the difference between the real and desired distributions, the proportional control takes 1.9995 s, and 482.79 units of energy (defined as $\int_0^\tau u(t)^2 dt$, where τ is the duration of control), whereas the bang-bang type control takes 2 s and 1351.83 units of energy. Bang-bang control requires significantly more energy as the large control input causes the probability distribution to overshoot the desired distribution when it is close to the uniform distribution. This results in rapid switches in the control input, as seen in the bottom left panel of Figure 2.

B. Type II neural population

Type II neuron models typically bifurcate through a Hopf bifurcation into the limit cycle regime. As an prototypical Type II neuron, here we consider the famous Hodgkin Huxley model [32], which undergoes a subcritical Hopf bifurcation with the periodic solution branch gaining stability through a saddlenode bifurcation of periodic orbits. We take the parameters from Chapter 2 in [33], with a constant applied current taken as 10mA. This results in a limit cycle with period $T = 14.638$ ms. We take the spatial grid size $d\theta = \pi/200$ rad, and time grid size $dt = 0.036595$ ms. We simulate equations (6) and (7) with both proportional control (13) and bang-bang control (14), with $k = 400$, $u_{max} = -u_{min} = 1.3$. Results for proportional and bang-bang control are shown in Figures 3 and 4, respectively.

We see that the both proportional and bang-bang control are able to transform the probability distribution into a uniform distribution over 5 time periods of the oscillator. To reach an L^2 norm of 0.001, the proportional control takes 52.59 ms, and 34.73 units of energy, whereas the bang-bang type control takes 142.1 ms and 240.11 units of energy. Bang-bang control requires significantly more energy and time to reach a desired L^2 norm, as the large control input again causes the probability distribution to overshoot the desired distribution when it is close to the uniform distribution. This results in rapid switches in the bang-bang control input, as can be seen in the bottom left panel of Figure 4.

To show the versatility of our control algorithm, we also include results for a Type II neural population, where the goal is to achieve a synchronized neural population from an initially desynchronized population. Here we take the initial distribution as $\rho(\theta, 0) = 1/(2\pi)$, and desired distribution as the von Mises distribution with $b = 26$. To implement the control algorithm, we consider the same parameters for Hodgkin Huxley model, but for numerical stability reduce the spatial grid size to $d\theta = \pi/500$ rad, and use the time grid size $dt = 0.014638$ ms. We simulate equations (6) and

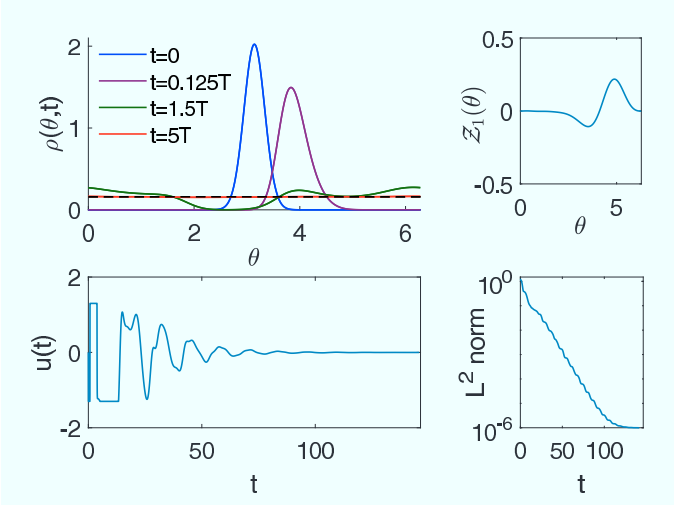

Fig. 3. Proportional control for a Type II neural population going from a synchronized to desynchronized state; here $k = 400$. In the top left panel, the colored (resp., black dashed) lines shows the probability distribution $\rho(\theta, t)$ (resp., $\rho_f(\theta, t)$) at various times. The top right panel shows the PRC, while the bottom panels show the control input and the L^2 norm (8) on a logarithm scale. Here $T = 14.638\ ms$.

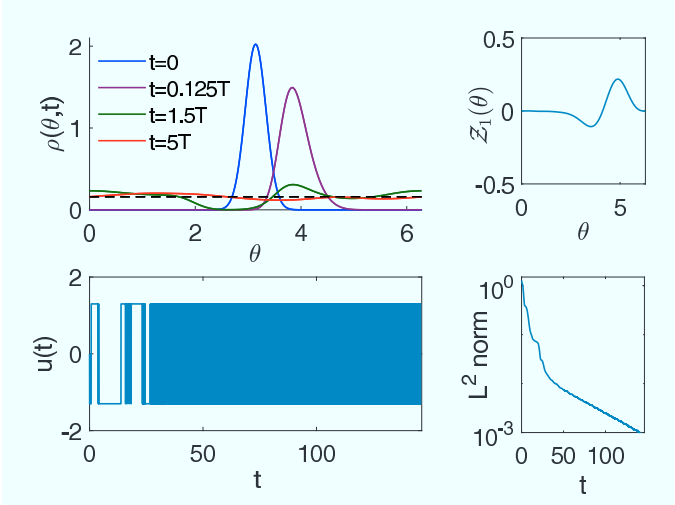

Fig. 4. Bang-bang control for a Type II neural population going from a synchronized to desynchronized state. In the top left panel, the colored (resp., black dashed) lines shows the probability distribution $\rho(\theta, t)$ (resp., $\rho_f(\theta, t)$) at various times. The top right panel shows the PRC, while the bottom panels show the control input and the L^2 norm (8) on a logarithm scale. Here $T = 14.638\ ms$.

(7) with bang-bang control (14), with $u_{max} = -u_{min} = 0.9$. Results are shown in Figure 5.

We see that the bang-bang control is able to transform the initial uniform distribution into the desired probability distribution over 15 time periods of the oscillator. To reach an L^2 norm (8) of 0.01, the bang-bang control takes 212.24 ms, and 171.91 units of energy. Here again, the large control input causes the probability distribution to overshoot the desired distribution when it is close to the desired distribution, resulting in rapid switches in the control input. We also see that the L^2 norm does not monotonically decrease with time, in contrast to the theory in Section III. This can be explained by the fact that the theory in Section III is valid for a continuous spatial and time domain, whereas our numerical results were obtained for a discretized domain, where the overshoots caused by the control input can momentarily increase the L^2 norm before eventually decreasing it. These overshoots can be decreased to some extent by decreasing the grid size.

V. CONCLUSIONS

In this article, we devised two related control algorithms which use proportional control and bang-bang control to change the synchrony properties of a poplulation of noise-free, identical, uncoupled neural oscillators all receiving the same control input. The algorithms are based on phase reduction, and use a population-level partial differential equation formulation to change the phase distribution of the neurons as desired. Motivated by the pathological neural synchronization present in patients suffering from essential and parkinsonian tremor, we used the algorithms to desynchronize initially synchronized populations of both Type I and Type II neurons. We also briefly showed that the algorithm can work in the other direction as well, i.e., in going from an initially desynchronized neural population to a synchronized one. This would be useful for applications mentioned in Section I, and also in control algorithms based on coordinated reset [9] in which neurons are synchronized within subpopulations but out of phase with other subpopulations.

In theory, the bang-bang control should decrease the L^2 norm more rapidly than the proportional control, since the time derivative of L^2 in bang-bang control is always less than that in proportional control. But since our numerical computations require discretization, the control input overshoots the probability distribution, resulting in rapid switches in the bang-bang control input. This not only results in slower decay rates of L^2 norm for the bang-bang control, but also leads to a non-monotonic decrease of L^2 norm in going from an initially desynchronized to a synchronized neural population. This inconsistency with theory can be reduced by decreasing the grid size, but that occurs at expense of an increased computational cost.

The algorithms described in this paper are quite flexible; for the systems considered in this paper, they have the potential to drive a system of neural oscillators from any initial phase distribution to any traveling-wave final phase distribution, as long as the combination of those distributions is non-degenerate. We conclude with remarks about the experimental implementation of these algorithms. Since they require knowledge of the current neuronal phase distribution, one would need to measure neuronal activity in order to back out this distribution in real time. This measurement would require good spatial and temporal resolution, so for both in vitro and in vivo experiments we suggest that the use of Micro-Electrode arrays (MEA) would be a good fit. Note that for in vivo experiments, fMRI and EEG are unlikely to

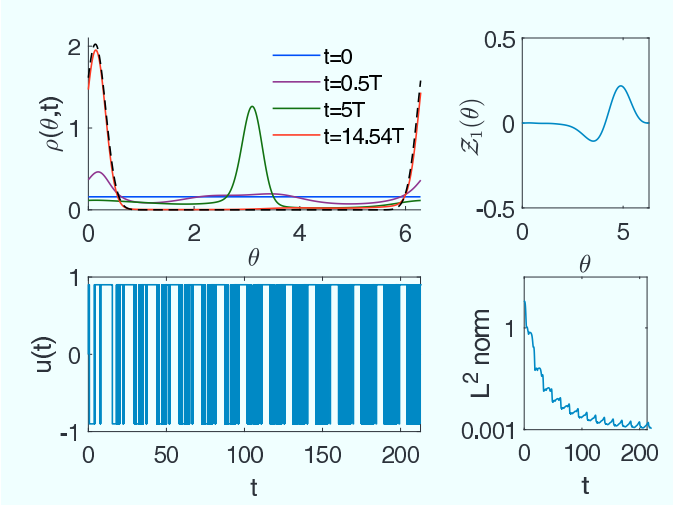

Fig. 5. Bang-bang type control for a Type II neural population going from a desynchronized to a synchronized state. In the top left panel, the colored (resp., black dashed) lines shows the probability distribution $\rho(\theta,t)$ at various times (resp., $\rho_f(\theta,t)$ at $t = 15T$). The top right panel shows the PRC, while the bottom panels show the control input and the L^2 norm (8). Here $T = 14.638\ ms$.

be the right tools since FMRI has poor temporal resolution, while EEG is susceptible to noise and poorly measures neural activity beneath the cortex. This work lays the foundation for a similar approach to neural control for more general models which include effects due to coupling, noise, and/or heterogeneity, topics which we are currently pursuing.

ACKNOWLEDGMENT

This work was supported by National Science Foundation Grant No. NSF-1635542. GF is partially supported by an Australian Research Council Discovery Project DP150100017.

REFERENCES

[1] C. Gray, P. König, A. Engel, and W. Singer, "Oscillatory responses in cat visual cortex exhibit inter-columnar synchronization which reflects global stimulus properties," *Nature*, vol. 338, no. 6213, pp. 334–337, 1989.

[2] R. Friedrich and M. Stopfer, "Recent dynamics in olfactory population coding," *Current Opinion in Neurobiology*, vol. 11, no. 4, pp. 468–474, 2001.

[3] G. Stent, "A physiological mechanism for Hebb's postulate of learning," *Proceedings of the National Academy of Sciences*, vol. 70, no. 4, pp. 997–1001, 1973.

[4] W. Klimesch, "Memory processes, brain oscillations and eeg synchronization," *International Journal of Psychophysiology*, vol. 24, no. 1, pp. 61–100, 1996.

[5] A. Kane, W. Hutchison, M. Hodaie, A. Lozano, and J. Dostrovsky, "Enhanced synchronization of thalamic theta band local field potentials in patients with essential tremor," *Experimental Neurology*, vol. 217, no. 1, pp. 171–176, 2009.

[6] A. Kühn, A. Tsui, T. Aziz, N. Ray, C. Brücke, A. Kupsch, G.-H. Schneider, and P. Brown, "Pathological synchronisation in the subthalamic nucleus of patients with Parkinson's disease relates to both bradykinesia and rigidity," *Experimental Neurology*, vol. 215, no. 2, pp. 380–387, 2009.

[7] J. Zhang, J. Wen, and A. Julius, "Optimal circadian rhythm control with light input for rapid entrainment and improved vigilance," in *Proceedings of the 51st IEEE Conference on Decision and Control (CDC)*. IEEE, 2012, pp. 3007–3012.

[8] D. Forger and D. Paydarfar, "Starting, stopping, and resetting biological oscillators: in search of optimum perturbations," *Journal of Theoretical Biology*, vol. 230, no. 4, pp. 521–532, 2004.

[9] P. Tass, "A model of desynchronizing deep brain stimulation with a demand-controlled coordinated reset of neural subpopulations," *Biological Cybernetics*, vol. 89, no. 2, pp. 81–88, 2003.

[10] C. Wilson, B. Beverlin, and T. Netoff, "Chaotic desynchronization as the therapeutic mechanism of deep brain stimulation," *Front. Syst. Neurosci.*, vol. 5, 2011.

[11] D. Wilson and J. Moehlis, "Optimal chaotic desynchronization for neural populations," *SIAM Journal on Applied Dynamical Systems*, vol. 13, no. 1, p. 276, 2014.

[12] J. Guckenheimer, "Isochrons and phaseless sets," *Journal of Mathematical Biology*, vol. 1, no. 3, pp. 259–273, 1975.

[13] J. Moehlis, E. Shea-Brown, and H. Rabitz, "Optimal inputs for phase models of spiking neurons," *Journal of Computational and Nonlinear Dynamics*, vol. 1, no. 4, pp. 358–367, 2006.

[14] A. Zlotnik, Y. Chen, I. Kiss, H. Tanaka, and J.-S. Li, "Optimal waveform for fast entrainment of weakly forced nonlinear oscillators," *Physical Review Letters*, vol. 111, no. 2, p. 024102, 2013.

[15] P. Tass, *Phase Resetting in Medicine and Biology: Stochastic Modelling and Data Analysis*. Springer-Verlag Berlin Heidelberg, 2007.

[16] D. Minors, J. Waterhouse, and A. Wirz-Justice, "A human phase-response curve to light," *Neuroscience Letters*, vol. 133, no. 1, pp. 36–40, 1991.

[17] B. Monga and J. Moehlis, "Optimal timing control of biological oscillators using augmented phase reduction," *Under Review*, 2017.

[18] T. Stigen, P. Danzl, J. Moehlis, and T. Netoff, "Controlling spike timing and synchrony in oscillatory neurons," *Journal of Neurophysiology*, vol. 105, no. 5, p. 2074, 2011.

[19] A. Nabi, T. Stigen, J. Moehlis, and T. Netoff, "Minimum energy control for in vitro neurons," *Journal of Neural Engineering*, vol. 10, no. 3, p. 036005, 2013.

[20] R. Snari, M. Tinsley, D. Wilson, S. Faramarzi, T. Netoff, J. Moehlis, and K. Showalter, "Desynchronization of stochastically synchronized chemical oscillators," *Chaos: An Interdisciplinary Journal of Nonlinear Science*, vol. 25, no. 12, p. 123116, 2015.

[21] P. Danzl and J. Moehlis, "Event-based feedback control of nonlinear oscillators using phase response curves," in *Decision and Control, 2007 46th IEEE Conference on*. IEEE, 2007, pp. 5806–5811.

[22] A. Nabi and J. Moehlis, "Nonlinear hybrid control of phase models for coupled oscillators," in *American Control Conference (ACC), 2010*. IEEE, 2010, pp. 922–923.

[23] P. Tass, "Effective desynchronization by means of double-pulse phase resetting," *EPL (Europhysics Letters)*, vol. 53, no. 1, p. 15, 2001.

[24] A. Winfree, "Biological rhythms and the behavior of populations of coupled oscillators," *Journal of Theoretical Biology*, vol. 16, no. 1, pp. 15–42, 1967.

[25] Y. Kuramoto, "Phase-and center-manifold reductions for large populations of coupled oscillators with application to non-locally coupled systems," *International Journal of Bifurcation and Chaos*, vol. 7, no. 04, pp. 789–805, 1997.

[26] E. Brown, J. Moehlis, and P. Holmes, "On the phase reduction and response dynamics of neural oscillator populations," *Neural Comp.*, vol. 16, pp. 673–715, 2004.

[27] Z. Lin, J.-L. Thiffeault, and C. R. Doering, "Optimal stirring strategies for passive scalar mixing," *Journal of Fluid Mechanics*, vol. 675, pp. 465–476, 2011.

[28] G. Froyland, C. González-Tokman, and T. M. Watson, "Optimal mixing enhancement by local perturbation," *SIAM Review*, vol. 58, no. 3, pp. 494–513, 2016.

[29] C. Shu and S. Osher, "Efficient implementation of essentially non-oscillatory shock-capturing schemes," *Journal of Computational Physics*, vol. 77, no. 2, pp. 439–471, 1988.

[30] ——, "Efficient implementation of essentially non-oscillatory shock-capturing schemes, ii," *Journal of Computational Physics*, vol. 83, no. 1, pp. 32–78, 1989.

[31] B. Ermentrout, "Type I membranes, phase resetting curves, and synchrony," *Neural Computation*, vol. 8, no. 5, pp. 979–1001, 1996.

[32] A. Hodgkin and A. Huxley, "A quantitative description of membrane current and its application to conduction and excitation in nerve," *The Journal of physiology*, vol. 117, no. 4, pp. 500–544, 1952.

[33] G. Ermentrout and D. Terman, *Mathematical Foundations of Neuroscience*. Springer-Verlag New York, 2010.